

Production and Correlations of Charged Particles with High P_t
in 200 GeV $\pi^\pm p$, $K^- p$ and pp Collisions

C. Bromberg, G. Fox, R. Gomez, J. Pine, S. Stampke, K. Yung
California Institute of Technology, Pasadena, California 91125

S. Erhan, E. Lorenz^(a), M. Medinnis, J. Rohlf, P. Schlein
University of California, Los Angeles, California 90024

V. Ashford^(b), H. Haggerty, R. Juhala^(c), E. Malamud, S. Mori
Fermi National Accelerator Laboratory, Batavia, Illinois 60510

R. Abrams, R. Delzenero, H. Goldberg, S. Margulies, D. McLeod, J. Solomon, R. Stanek
University of Illinois at Chicago Circle, Chicago, Illinois 60680

A. Dzierba, W. Kropac^(d)
Indiana University, Bloomington, Indiana 47401

ABSTRACT

Results are presented on the production of single charged particles with transverse momentum in the range 0.8 to 4.5 GeV/c in $\pi^\pm p$, $K^- p$ and pp collisions at 200 GeV and on correlations between the trigger particle and particles with opposite azimuthal angle.

High transverse momentum (P_t) production of hadrons is thought to proceed through hard constituent scattering. Earlier results¹ on collective high P_t phenomena (i.e., "jets") were obtained by us using a large-aperture calorimeter-triggered multi-particle spectrometer at The Fermi National Accelerator Laboratory (Experiment E260). In this Letter, we present production cross sections for single charged particles with $0.8 < P_t < 4.5$ Gev/c and at 90° in the C.M., produced in 200 Gev π^-p , π^+p and pp collisions. Positive to negative charge ratios of \hat{C} erenkov-identified secondary particles are given, as well as correlations between the charge of associated "away-side" particles (those on the opposite side in azimuth from the trigger particle) and the trigger particle species.

Details of the spectrometer and of the single-particle trigger used for the data presented here are found in ref. 1. We note here that, in order to understand the properties of the trigger bias, data were recorded for several different calorimeter bias settings, corresponding to P_t lower limits as low as 1.75 Gev/c and as high as 3.0 Gev/c. In general, a particle with P_t below the trigger threshold can trigger the calorimeter in any of three ways: (a) The observed energy loss in the calorimeter is an upward fluctuation; (b) the magnetic deflection can increase a particle's laboratory angle and hence its apparent P_t ; or (c) an additional particle deposits energy in the same calorimeter cell. (a) and (b) are adequately accounted for in a Monte Carlo acceptance calculation, while (c) can be corrected for by observing any accompanying charged particles in the spectrometer. Accompanying neutral particles are less frequent and can be estimated. Further details on these points will be reported elsewhere², although we should comment here that in the various ratios presented below, such corrections tend to cancel.

The 22-cell \hat{C} erenkov counter \hat{C}_1 , shown in ref. 1, was used to identify secondary particles wherever possible. For 70% of the data, \hat{C}_1 was filled

with air (K threshold ≈ 21 Gev/c) and the remainder of the time filled with a 2:1 helium-air mixture (K threshold ≈ 32 Gev/c). At ~ 0.1 radian in the laboratory (90° in the CM), we could therefore uniquely identify π 's and a mixed K-p sample with P_t up to 3.2 Gev/c; we could uniquely identify p's (and also \bar{p} 's) and a mixed π -K sample with P_t greater than 2.1 Gev/c. Since $\beta = 1$ particles produced an average of eight photo-electrons in air, pulse height information could be used to identify π 's with $P_t > 2.1$ Gev/c in these data; with helium-air, corrections of up to 10-15% were necessary for π -background in the K-p sample.

Fig. 1(a) shows our measurement of the inclusive charged particle cross section for pp collisions. The results agree with the corresponding data from the Chicago-Princeton (CP) collaboration³. Fig. 1(b) shows our ratio of the pp cross section to the corresponding π^-p charged-particle cross section. This ratio is almost identical to the $(pp \rightarrow \pi^0)/(\pi^-p \rightarrow \pi^0)$ ratio of Donaldson et al.⁴ Moreover, our ratio of $(\pi^+p)/(\pi^-p)$, which is seen in Fig. 1(c) to be P_t -independent at a value near unity, also agrees with the Donaldson et al. results for π^0 production. The fall-off of our pp/π^-p ratio in Fig. 1(b) shows that there is a crossover of πp and pp single particle cross sections near $P_t \approx 3$ Gev/c.

A summary of various ratios of trigger particle charge components in pp interactions to those in π^-p interactions is shown in Figs. 2(a-b); the same ratios for π^+p to π^-p interactions are shown in Figs. 2(c-d). The solid curves show fits to the data of the function $(1 - x_\perp)^n$, where $x_\perp = P_t/P_t^{\max}$. Since the presence of baryons in the final state may complicate the interpretation of these results, the dashed curves in Figs. 2(a-b) show the effects on these ratios of removing p's and \bar{p} 's from the final states. Since, as discussed below, the final state baryon components in π^-p and π^+p interactions are consistent with being nearly identical, the ratios displayed in Figs. 2(c-d) are essentially the ratios for $\pi + K$ production only. These latter ratios are seen to vary very slowly, if

at all, with P_t .

Fig. 3(a) shows the (+/-) trigger charge ratio for pp, π^+p and K^-p interactions vs. P_t . The pp results agree well with those of CP³. Despite differences in the initial-state quark content, π^+p is seen to have the same behavior as pp and K^-p is similar to π^-p . Both the π^+p and π^-p results are seen to be correctly predicted by the early QCD approximation of Field and Feynman⁵ (FF), although a quark-fusion⁶ constituent-interchange⁷ (CIM) model parametrization by Chase and Stirling⁸ (CS) is seen to disagree completely with the π^+p result. The CIM term alone in CS fits neither π^+p nor π^-p .

The results for the identified trigger particles are shown in Figs. 3(b-d). The proton-beam data are seen to agree with the analogous results from CP³ and with the FF and CS predictions for $pp \rightarrow \pi + X$. We note that the ratio $(p + K^+)/(\bar{p} + K^-)$ is much larger than the π^+/π^- ratio for the proton-beam data, whereas for the π^- -beam the two ratios are comparable. This is presumably due to the fact that protons contain none of the valence quarks necessary to form \bar{p} or K^- in the denominator of the first ratio. The p/\bar{p} ratio for π^- -beam is seen to be close to unity, as compared with the larger p/\bar{p} ratio of 6 or more for proton-beam³. This presumably also results from the valence-quark content of the initial-state. Finally, Fig. 3(d) shows the proton/meson production ratios for the three reactions. None of the ratios appears to depend appreciably on P_t . The ratio for the lower statistics π^+p data (not shown) agrees with the π^-p data.

We turn now to the charge correlations between "away-side" hadrons and the type of trigger particle⁹. We define $R_a(h)$ as the away-side positive to negative charge production ratio for all charged particles with CM production angle $45^\circ < \theta < 90^\circ$ and which lie in a $\pm 45^\circ$ azimuthal wedge opposite the trigger particle; a is the incident beam particle and h is the trigger particle. In Fig. 4 we plot $R_a(\pi)$ and $R_a(K + p)$ for two different regions of $x_e = -\hat{p}_1^{\text{away}} \cdot \hat{p}_1^{\text{trig}} / p_1^{\text{trig}}$. We note that there is a pronounced dependence on x_e and, furthermore, that R_a appears to depend only on the charge of the trigger particle and not on its type,

in agreement with QCD predictions¹⁰.

In a simple quark fragmentation model, a negative trigger in a π^-p collision increases the likelihood that the away quark came from a proton, while a positive trigger suggests that the away quark came from the π^- . Thus, we expect $R_{\pi^-}(h^+) < R_{\pi^-}(h^-)$, as observed. Further, since a minus trigger can come either from the d-quark in the incident proton or the d or \bar{u} quarks in the π^- , the denominator in $R_{\pi^-}(h^-)$ will be enhanced somewhat and we expect $R_{\pi^-}(h^-) < R_p(h^+)$, which is also seen. Thus the general pattern of the $x_e > 0.4$ data in Fig. 4 agrees with the qualitative predictions of the simple parton model, although the differences between $R_p(h^-)$ and $R_p(h^+)$ are larger than expected. A possible explanation is that all the residual valence quarks (those that do not directly participate in the hard scatter) influence the charge correlations on the far side. In other words, we are probably seeing contamination from the forward jet¹¹. Whereas $x_e > 0.4$ should be large enough to eliminate contamination from the large $x_{||}$ component of the forward jet, it is not large enough to eliminate the low $x_{||}$ component. A detailed understanding of the quantitative features of the correlation data will have to await experiments at higher P_t , so that the contamination from the forward jet can be reduced.

We are grateful for the assistance given us by the staffs of the Accelerator Division, the Meson Department and the Research Services Department at Fermilab. We thank B. Combridge, R. Field and A. Pagnamenta for useful discussions. This work was supported in part by the U.S. National Science Foundation (UCLA and UICC) and the U.S. Department of Energy (Caltech, Fermilab and Indiana) and the University of Illinois Research Board.

Footnotes and References

- (a) Visitor from the Max Planck Institut für Physik und Astrophysik, Munich
- (b) Presently at Brookhaven National Laboratory, Upton, N.Y.
- (c) Presently at McDonnell Douglas Corporation, St. Louis, MO.
- (d) Presently at Hughes Aircraft Corporation, Los Angeles, CA.
- (1) C. Bromberg et al., Phys. Rev. Letters 38, 1447 (1977); Nucl. Phys. B134, 189 (1978); Proceedings of the VIII International Symposium on Multiparticle Dynamics, Kayserberg, France, pp. B89 (June 1977); and Jets Produced in π^- , π^+ and Proton Interactions at 200 Gev on Hydrogen and Aluminum Targets, Phys. Rev. Letters (in press - 1979)
- (2) See also Ph.D. theses by M. Medinnis (UCLA) and R. Stanek (UICC)
- (3) D. Antreaseyan et al., Phys. Rev. Lett. 38, 112, 115 (1977)
- (4) G. Donaldson et al., Phys. Rev. Lett. 36, 1110 (1976)
- (5) R. Field and R. P. Feynman, Phys. Rev. D15, 2590 (1977)
- (6) P. V. Landshoff and J. C. Polkinghorne, Phys. Rev. D10, 891 (1974)
- (7) R. Blankenbecler, S. J. Brodsky and J. Gunion, Phys. Rev. D12, 3469 (1975)
- (8) M. K. Chase and W. J. Stirling, Nucl. Phys. B133, 157 (1978)
- (9) Similar data from pp collisions in different kinematic regions are available from CERN {K. H. Hansen Proceedings of the XIX International Conference on High Energy Physics, Tokyo, Japan, p. 177 (1978)} and Fermilab {R. J. Fisk et al., Phys. Rev. Lett. 40, 984 (1978)}
- (10) R. P. Feynman, R. D. Field and G. C. Fox, Phys. Rev. D18, 3320 (1978)
- (11) Theoretical descriptions of our correlation data should take into account our θ selection on the away side; the contribution of away-side quarks may be enhanced with respect to that of gluons because particles are selected in the forward hemisphere; this may help explain the large value of $R_p(h^-)$. See M. K. Chase, Phys. Lett. 79B, 114 (1978)

Figure Captions

- Figure 1. (a) Inclusive invariant cross sections vs. P_t for $pp \rightarrow$ charged particle + X. Chicago-Princeton points are from ref. 3;
 (b) Ratio of cross section in (a) to that for $\pi^-p \rightarrow$ charged particle + X. Dashed curve is from ref. 4;
 (c) Ratio of π^+p to π^-p single charged particle cross sections.
- Figure 2. (a-b) Ratios of pp to π^-p single particle cross sections for indicated charge trigger particles. Solid curves are fits of $(1 - x)^n$ to the data with $P_t > 1\text{GeV}/c$; the exponents n are shown; they have statistical uncertainty of ± 0.2 . Dashed curves correspond to meson final states only.
 (c-d) Same as (a-b) except for π^+p and π^-p reactions. In this case the statistical uncertainties on the exponents are ± 0.4 .
- Figure 3. (a) Trigger particle charge production ratio vs. trigger particle P_t for pp and $\pi^\pm p$ reactions. Open symbols are from ref. 3. FF and CS curves are from refs. 5 and 8.
 (b) Same as (a), except for identified final state trigger particles in pp reactions.
 (c) Same as (b) except for π^-p reactions.
 (d) Baryon/meson production ratios for indicated reactions.
- Figure 4. The away-side charge production ratio for all away-side charged particles in the θ - ϕ acceptance region described in the text, for the indicated trigger particle types (a) for π^- -beam; (b) for proton-beam particle.

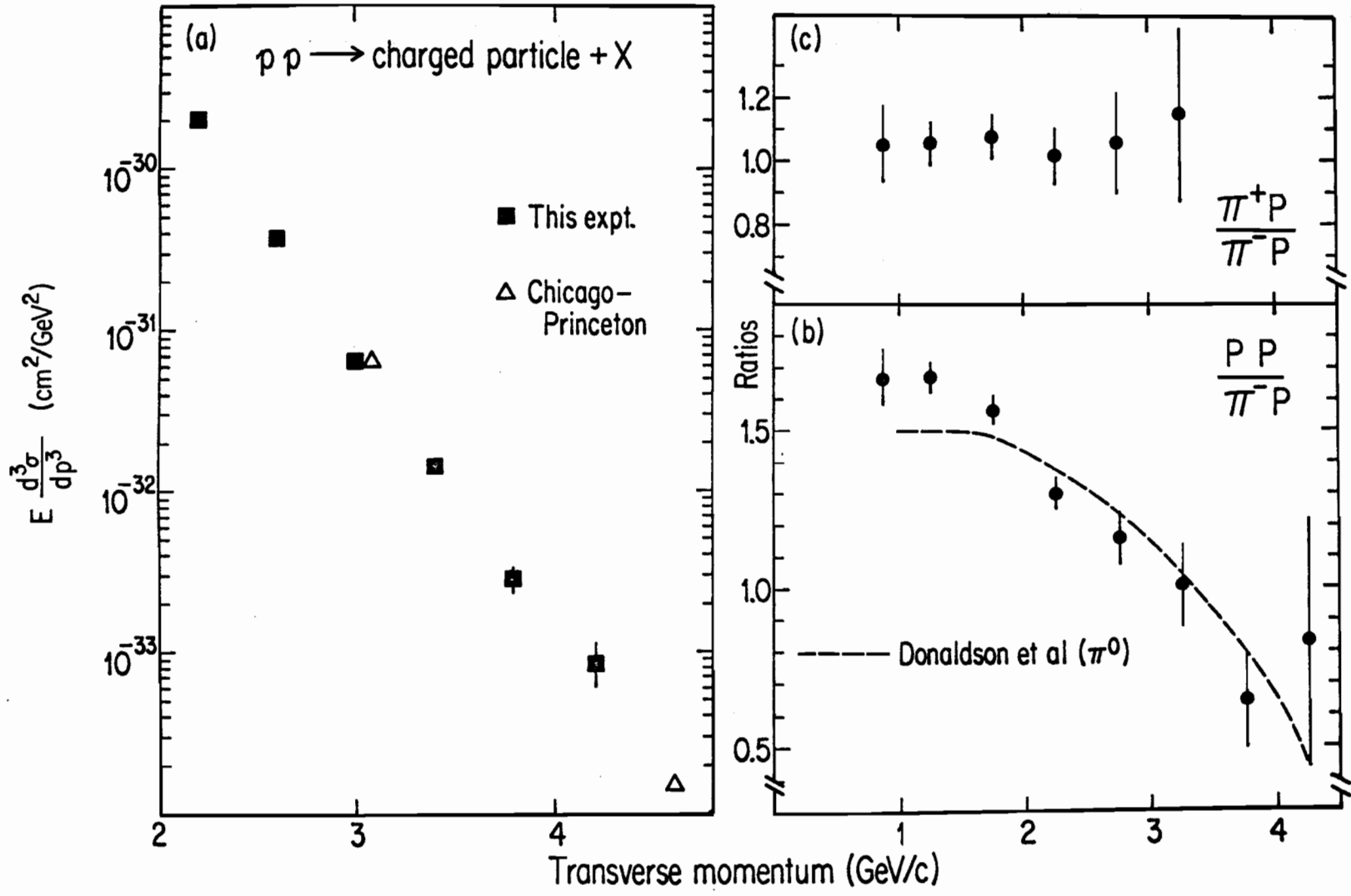


Figure 1

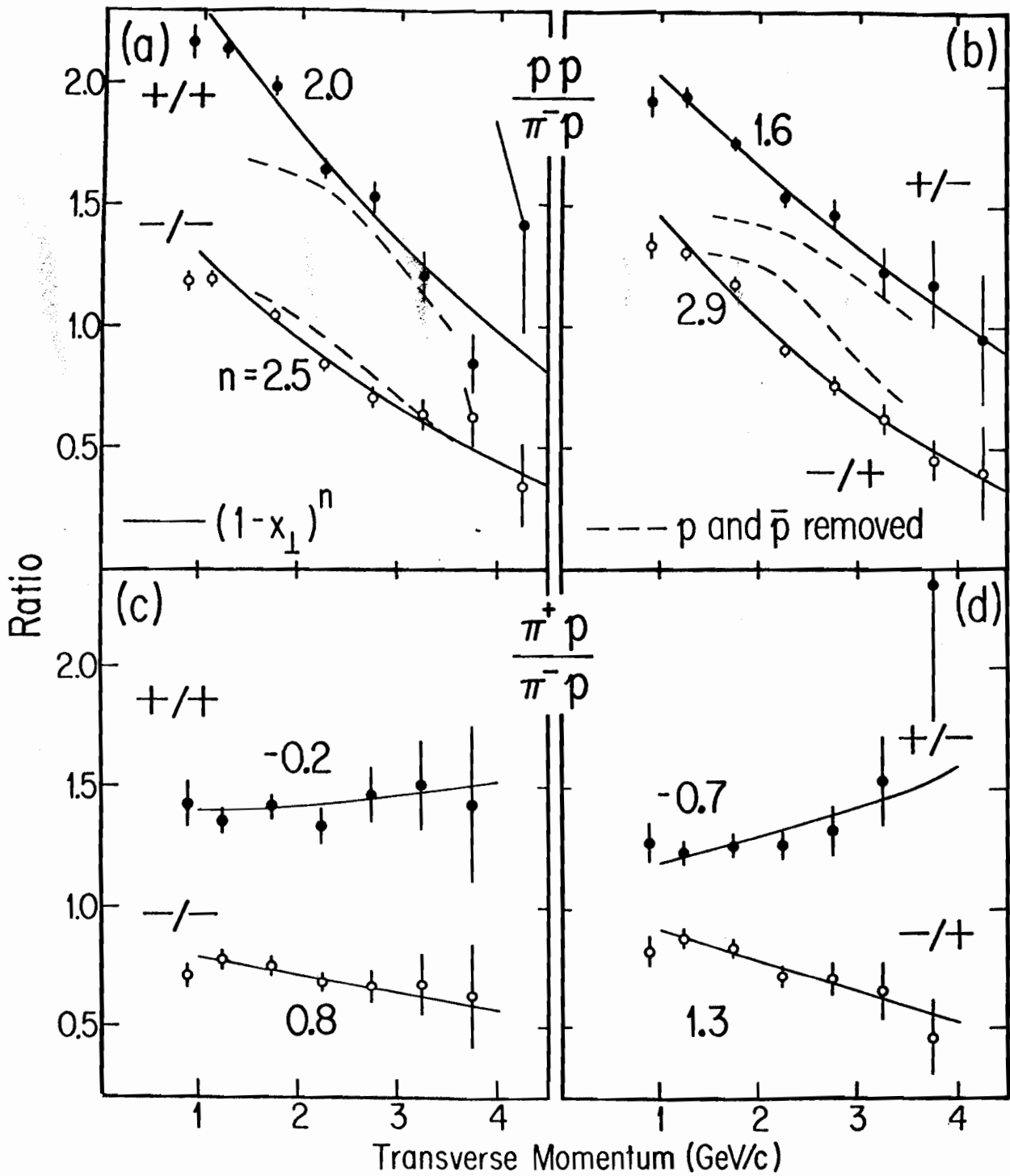


Figure 2

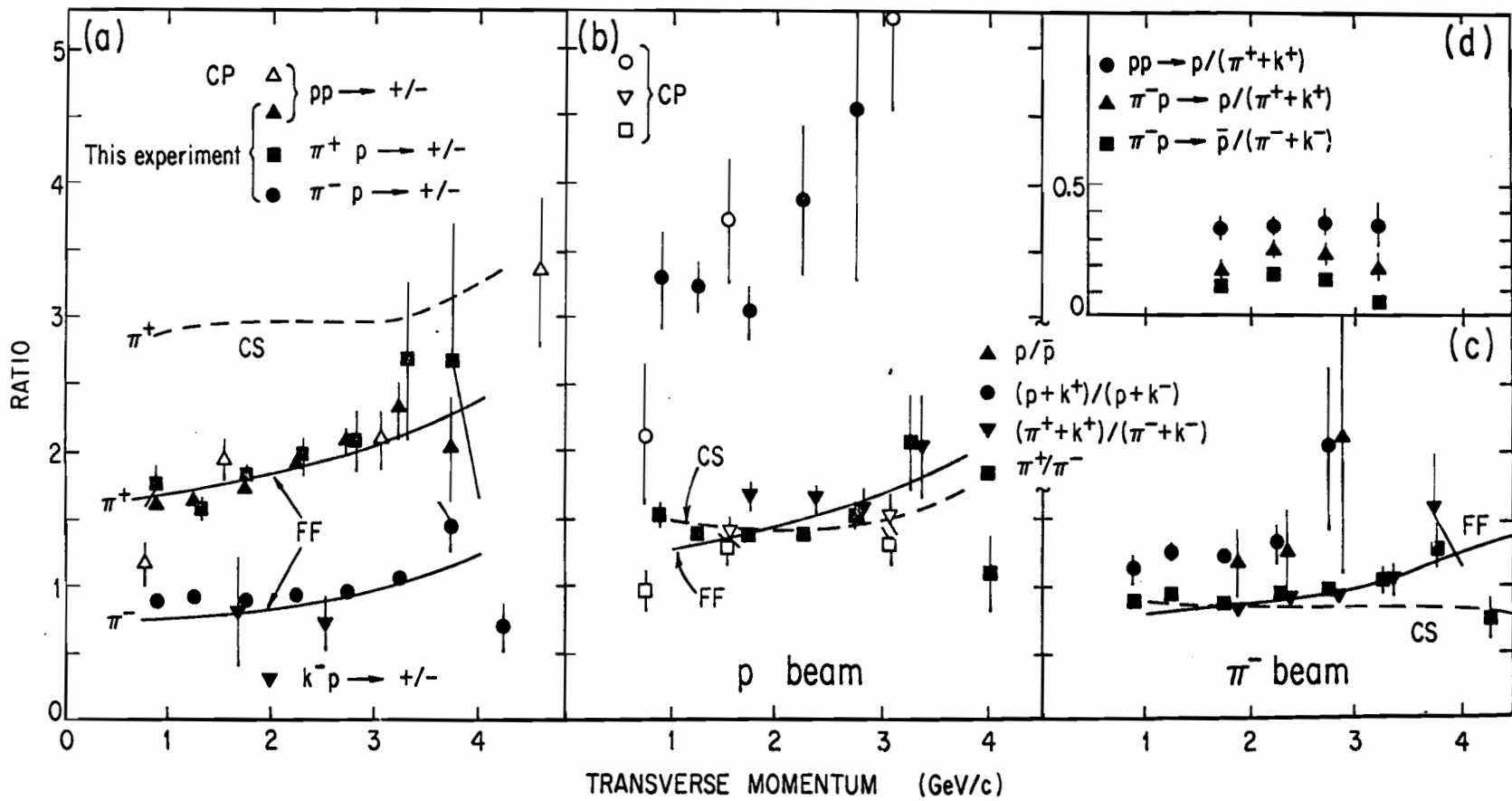


Figure 3

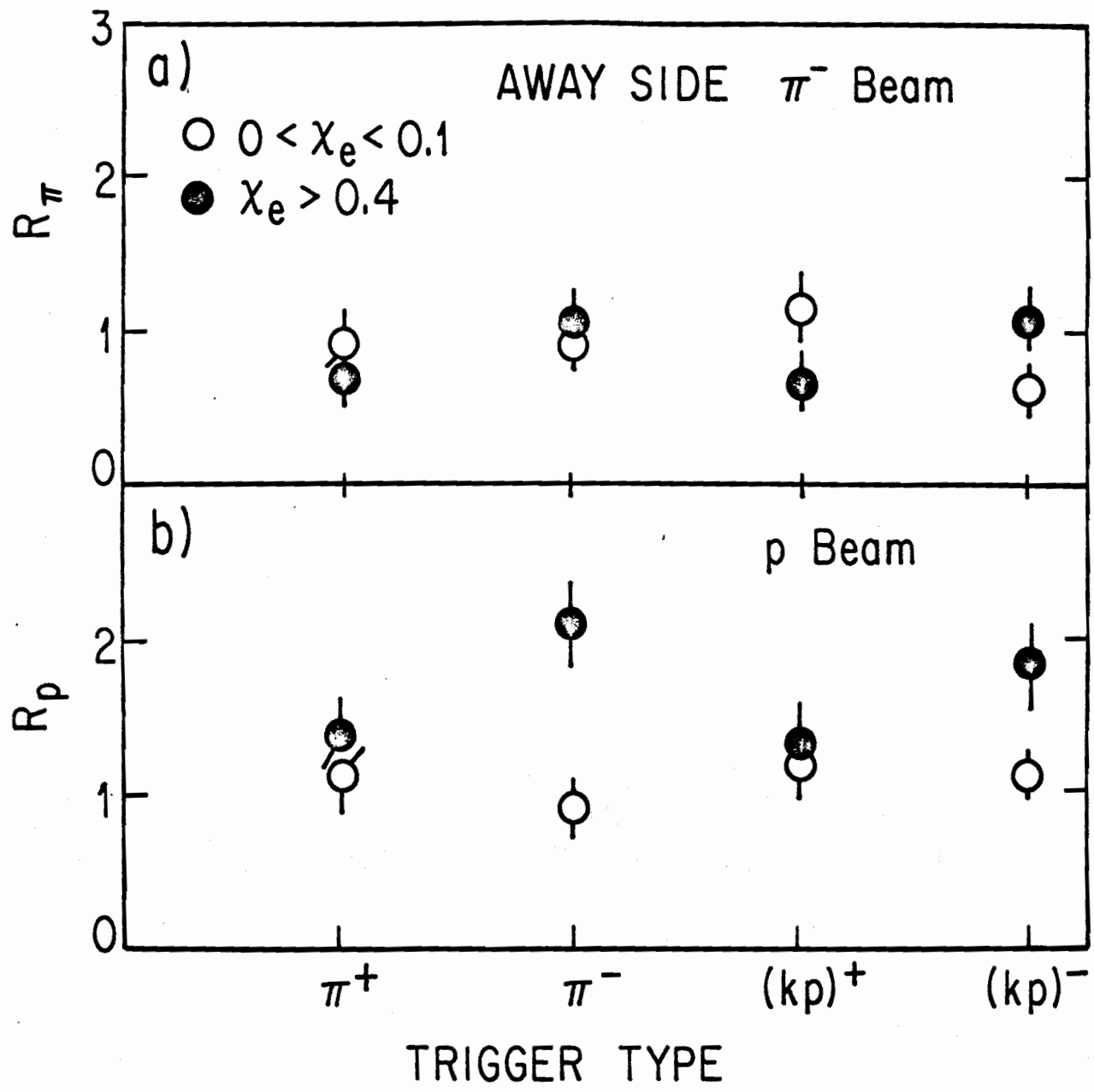


Figure 4